


 Cite this: *RSC Adv.*, 2020, 10, 24507

Dual responsive oligo(lysine)-modified Pluronic F127 hydrogels for drug release of 5-fluorouracil†

Peihong Li, Xueyan Dai, Lijie Qu, Yanlong Sui and Chunling Zhang *

Peptide-containing hydrogels have become a research hotspot due to their unique secondary structure and biocompatibility. Herein, we used amino-terminated F127 as a macroinitiator to initiate the ring-opening polymerization of L-lysine(z)-NCA, and the obtained oligo(lysine)-modified F127 (FL) had degrees of polymerization of lysine of 2, 5, and 8. The results showed that the FL hydrogels had reversible temperature-dependent sol–gel transitions, and the introduction of lysine increased the critical gel temperature. In the dilute solution of FL, the micelle size increased and aggregated as the pH increased; the micelle grew into a rod-like shape under alkaline conditions. Scanning electron micrographs showed that the interior of the FL hydrogel had a more complete porous structure. The FL-2 hydrogel loaded with 5-fluorouracil exhibited an approximately linear release trend within 12 h and has good biocompatibility. Therefore, FL hydrogels have potential applications in the field of biomedicine.

 Received 9th April 2020
 Accepted 21st June 2020

DOI: 10.1039/d0ra03207g

rsc.li/rsc-advances

Introduction

Intelligent hydrogels have attracted considerable attention because of their capability to change volume and properties in response to external stimuli.^{1–3} Temperature- and pH-responsive hydrogels are typical examples. The copolymer poly(ethylene oxide)-*b*-poly(propylene oxide)-*b*-poly(ethylene oxide) (PEO–PPO–PEO), which is also known as Pluronic® or poloxamer, is a commonly used temperature-responsive hydrogel material.^{4,5} The gelation transition of PEO–PPO–PEO hydrogels is related to temperature and concentration, and each hydrogel has a fixed critical micelle temperature (CMT) and a critical micelle concentration (CMC). For example, 20 wt% F127 has a gelation temperature of 25 °C. The PEO–PPO–PEO molecular chain is soft and has good hydrophilicity, biosafety, and biocompatibility.⁶ The micelles and hydrogels formed by this molecular chain have been used in drug delivery^{7,8} and tissue engineering,^{9,10} particularly injectable hydrogel drug delivery systems.^{11–13} pH-responsive hydrogels with ionizable acidic or basic pendant groups result in pH-induced changes in volume, mass, and elasticity.¹⁴ In anionic networks, ionization occurs when the ambient pH is above the acid group's characteristic pK_a, resulting in an increase in the amount of fixed charge, network hydrophilicity, and electrostatic repulsion between the chains. However, the protonation of the ionized acidic groups upon the pH reduction of an aqueous solution decreases the content of mobile counterions inside the matrix,

the strength of the electrostatic repulsions of the chain segments, and the volume shrinkage of the hydrogel. Cationic networks exhibit an opposite trend. When pK_a of the cationic pendant groups is higher than the environmental pH, the hydrophilicity of the network increases, and the hydrogel starts to swell.^{15,16}

Some natural components are introduced into the hydrogel system, such as polypeptides, to improve the biocompatibility of synthetic hydrogels and impart bio-functionality.¹⁷ The secondary structure of polypeptides (*e.g.*, α -helix, β -sheet) can improve the stability and mechanical properties of hydrogels^{18,19} and enable response to environmental stimuli.^{20,21} Even certain polypeptides have inherent antibacterial and cell adhesion properties.¹⁰ Peptide-containing hydrogels are adopted in drug delivery, cell scaffolds, and wound repair. In this paper, we introduced several repeating units of lysine at the end of F127. Since an excessive amount of lysine prevented the gelation of F127, the degrees of polymerization (DPs) of lysine were controlled to be 2, 5, and 8. Oligo(lysine) formed an α -helix conformation under alkaline conditions. The addition of oligo(lysine) not only increased the gelation temperature but also imparted pH sensitivity. We also studied the controlled release of anticancer drug 5-fluorouracil (5-FU) by hydrogel before and after modification.

Experimental section

Materials

Pluronic F127 and methane sulfonyl chloride were obtained from Sigma-Aldrich. *N*_ε-Benzoyloxycarbonyl-L-lysine (L-lysine(z)) was purchased from Energy Chemical. Polyethylene glycol (PEG4000), triethylamine, triphosgene, trifluoroacetic acid

School of Materials Science and Engineering, Jilin University, Changchun, 130022, P. R. China. E-mail: clzhang@jlu.edu.cn

† Electronic supplementary information (ESI) available: FT-IR and ¹H NMR spectra of L-lysine(z)-NCA, CMT and CGT of hydrogels. See DOI: 10.1039/d0ra03207g



(TFA), 5-FU (98%), and trifluoroacetic acid-d (TFA-d) were obtained from Aladdin. Moreover, 33% HBr/acetic acid solution was acquired from J&K Chemical. Dichloromethane, tetrahydrofuran (THF), *N,N*-dimethylformamide (DMF), chloroform, petroleum ether, ammonium hydroxide solution, potassium dihydrogen phosphate, and sodium hydroxide were purchased from Beijing Chemical Works. Dimethyl sulfoxide-d₆ (DMSO-d₆) was obtained from CIL.

Synthesis of oligo(lysine)-modified F127 (FL)

First, the amino-terminated F127 was prepared following literature.¹⁸ Amination of F127 was confirmed by ninhydrin colorimetry. The *N*-carboxyanhydride form of L-lysine(z) (L-lysine(z)-NCA) was then prepared.²² Briefly, 2.0 g of L-lysine(z) was dissolved in 50 mL of THF, and the temperature was raised to 50 °C. Next, 2.0 g of triphosgene was added in three portions, and the reaction solution turned into a transparent gel that disappeared in approximately 5 min. The reaction was deemed completed after the solution completely cleared. The solution was poured onto cold petroleum ether to precipitate after its temperature decreased to room temperature. The product was dissolved in THF, reprecipitated once, and lyophilized. L-lysine(z)-NCA, 60% yield: ¹H NMR (DMSO-d₆ with 0.03% v/v TMS, 600 MHz): δ 9.07 (s, 1H), 7.33 (m, 5H), 7.24 (t, 1H, *J* = 5.5 Hz), 5.00 (s, 2H), 4.43 (m, 1H), 2.98 (q, 2H, *J* = 6.5 Hz), 1.69 (m, 2H), 1.41 (q, 2H, *J* = 6.8 Hz), 1.28 (m, 2H). See Fig. S1† for details.

The amino-terminated F127 was used as a macroinitiator to initiate the ring-opening polymerization (ROP) of L-lysine(z)-NCA in a mixture of DMF and chloroform (1 : 2 v/v). The reaction was conducted at 25 °C for 24 h, and the solution was poured onto cold petroleum ether for precipitation. The obtained polymer was dissolved in TFA, and 33% HBr/acetic acid solution was added to complete the deprotection reaction of L-lysine(z). The reaction was continued for 6 h under ice bath conditions, and the solution was precipitated in cold petroleum ether. The product was dialyzed (MWCO = 500) against deionized water for 24 h and lyophilized to obtain FL.

FT-IR spectra were obtained using a Fourier transform infrared spectrometer (FT-IR; Nexus 670, Nicolet) by using KBr disks. Thirty-two scans at a resolution of 4 cm⁻¹ were conducted to record the spectra. ¹H NMR spectra were obtained using a nuclear magnetic resonance spectrometer (NMR; Avance 600, Bruker) with DMSO-d₆ and TFA-d as solvent. The molecular weight and molecular weight distribution of the polymers were measured by gel permeation chromatography (GPC; Breeze, Waters) with THF as eluent at a flow rate of 1.0 mL min⁻¹. The secondary structure present in 0.1 wt% oligo(lysine)-modified PEG4000 aqueous solution was probed using a circular dichroism spectroscopy (CD; Chirascan, Applied Photophysics).

Preparation and characterization of hydrogels

Formulated FL solutions with a mass fraction of 4.0–24.0% were stored at low temperature until completely dissolved. The FL hydrogels were obtained by heating the FL solutions to 37 °C in a water bath and held for 12 h.

A differential scanning calorimeter (DSC; Q20, TA Company) was used to measure the CMT and CGT,²³ which was heated from 4 °C to 40 °C at 1 °C min⁻¹ under a nitrogen atmosphere. The rheological properties of the hydrogel were studied with a rheometer (AGES-G2, TA Company), using 25 mm parallel plates at 37 °C. The size and morphology of the micelles in the 0.05 wt% polymer solution at 20 °C were characterized by dynamic light scattering (DLS; DAWN EOS, Wyatt Technology) and transmission electron microscopy (TEM; JEM-2100F, JEOL). The DLS measurement was repeated three times and the average value was calculated. Scanning electron microscopy (SEM; XL-30 ESEM FEG, FEI Company) with an acceleration voltage of 10 kV was utilized to observe the interior morphologies of lyophilized hydrogels after sputter coating with gold.

Drug release studies

F127 and FL-2 hydrogels with 20 wt% were used as carriers, and 5-FU was used as a model drug. Each group contained 2.0 g hydrogel and 5 mg 5-FU. The sample was not removed from the vial. They were then placed in 100 mL of phosphate buffer solution (PBS) and incubated at 37 °C. The absorbance of PBS was measured using an ultraviolet spectrophotometer (UV-6100s, MAPADA) at each fixed time interval. The corresponding concentration of 5-FU was calculated by the following equation:

$$A = 52.72c + 0.008 \quad (R^2 = 0.999),$$

where *A* is the absorbance and *c* is the concentration. This equation calculates the cumulative release percentage (CR%). The *in vitro* drug release experiment was repeated five times, and the average values were obtained to plot the cumulative release curve.

In vitro cytocompatibility evaluations

Mouse embryonic fibroblasts cell line (NIH/3T3) was purchased from American Type Culture Collection (ATCC). NIH/3T3 cells were cultured in Dulbecco's modified Eagle's medium (DMEM, Gibco) containing 10% Foetal Bovine Serum (FBS, Gibco) and 1% penicillin/streptomycin, and incubated at 37 °C in a humidified atmosphere with 5% CO₂.

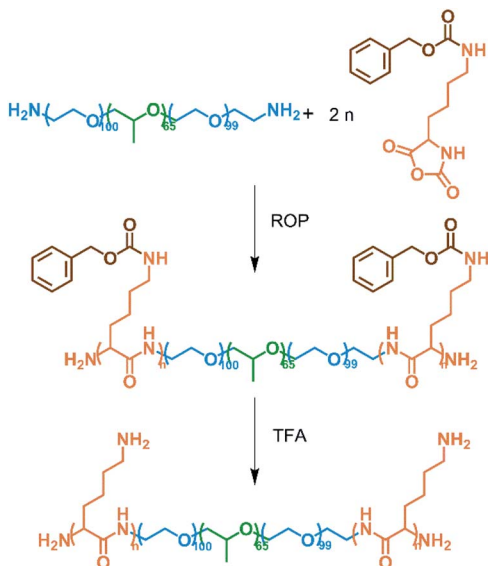
NIH/3T3 cells were plated in 96-well plates (1 × 10⁴ cells per well) and allowed to adhere for 10 h. Remove the medium and replace it with medium containing different concentrations of F127 and FL-2. Fresh medium was used as a control group. The cells were treated with methyl thiazolyl tetrazolium (MTT, Sigma-Aldrich) after 24 and 48 h. Absorbance at 490 nm was measured using a microplate reader (Spark, Tecan). The cell viability was calculated by the following equation:

$$\text{Cell viability (\%)} = (A/A_{\text{control}}) \times 100\%,$$

where *A* and *A*_{control} are the absorbance of the test group and the control group, respectively.

The NIH/3T3 cells were encapsulated in 20% F127 hydrogel and FL-2 hydrogel. The cells were first suspended in PBS and then mixed with PBS of F127 or FL-2 at about 5 °C. This mixture





Scheme 1 Synthetic route of FL polymer. The amino-terminated F127 initiates the ring-opening polymerization of L-lysine(z)-NCA and the deprotection reaction in the environment of trifluoroacetic acid.

was put into 6-well plate (2×10^5 cells per well) and quickly formed cell-loaded hydrogel. The hydrogel was incubated at 37°C for 5 min, and 4 mL of medium was added to each well. Cells were stained with Live/Dead staining (calcein-AM/PI, Meilunbio) after 24 and 48 h, and the morphology and viability of the cells were observed by a fluorescent inverted microscope (TE2000, Nikon).

Results and discussion

Polymerization and deprotection of FL

The amino-terminated F127 was used as a macroinitiator to initiate the ROP of L-lysine(z)-NCA and then deprotected in a TFA environment to obtain the FL polymer (Scheme 1). Fig. 1

shows the FT-IR and ^1H NMR spectra of the reactants and products. In Fig. 1(a), characteristic peaks at 3340, 2940–2860, and 1110 cm^{-1} were assigned to the amide bond, methylene group, and ether bond, respectively. The peak at 1857 cm^{-1} represented the five-membered cyclic anhydride of NCA, and it disappeared in oligo[lysine(z)]-modified F127 and FL, indicating that the L-lysine(z)-NCA had polymerized. The FL showed the peak of primary amine at 1685 cm^{-1} . The characteristic peak of phenyl group at 744 cm^{-1} disappeared, meaning that the deprotection reaction had been completed. Meanwhile, in the ^1H NMR spectra of FL, the peaks of the protecting group benzylloxycarbonyl at 7.42, 5.48, and 7.39 ppm disappeared, and the peak of the amino group appeared at 6.97 ppm (Fig. 1(b)). Therefore, the protecting group had been removed, and the chains were not broken.

Polymers with different molecular weights were prepared by controlling the distribution ratio. Three groups of FL were obtained and named FL-2, FL-5, and FL-8. Table 1 presents the molecular weight and polydispersity measured by GPC. The results show that the molecular weight of the polymer increased with the proportion of L-lysine(z)-NCA. Polydispersity values were between 1.36 and 1.55, representing unimodal distribution and low polydispersity.

Secondary structure of oligo(lysine)

The secondary structure of FL could not be detected probably because the molecular weight of the main chain F127 was too large, and the content of the terminal oligo(lysine) was relatively small. Oligo(lysine)-modified PEG4000 was prepared by the same procedure as in the preparation of FL (the DP of lysine is 5) to observe the changes in the oligo(lysine) secondary structure. Fig. 2 presents the CD spectra of oligo(lysine)-modified PEG4000 solution at pH 3.0, 7.4, and 11.0. The secondary structure of the polymer containing oligo(lysine) was not characterized under neutral and acidic conditions. By contrast, the characteristic negative ellipticity of an α -helix was observed at 204 and 220 nm in an alkaline solution.^{20,24,25} These results

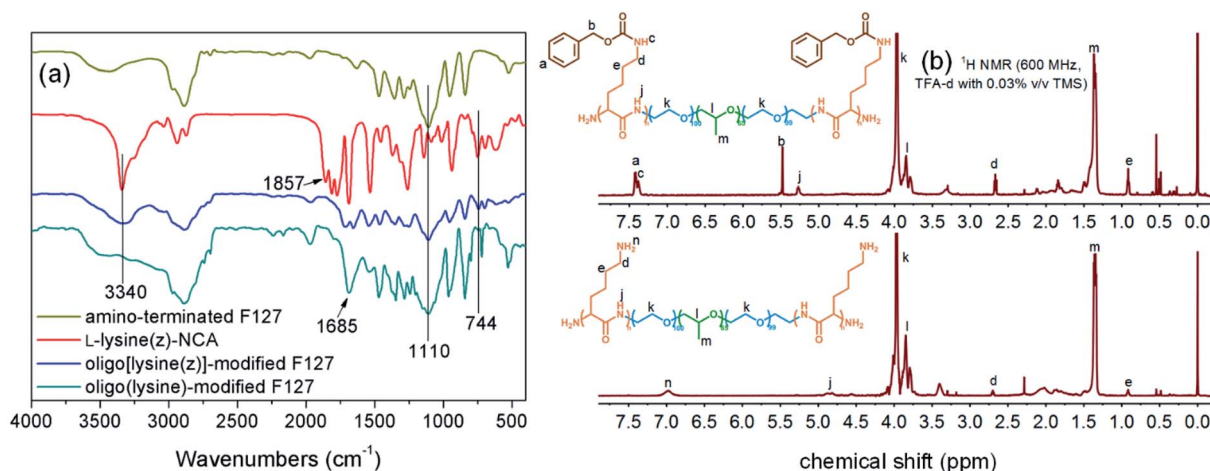


Fig. 1 (a) FT-IR spectra of amino-terminated F127, L-lysine(z)-NCA, oligo[lysine(z)]-modified F127, and FL; (b) ^1H NMR spectra of oligo[lysine(z)]-modified F127 and FL.



Table 1 Molar ratio, molecular weight, and polydispersity of FL polymers

| Sample | Molar ratio (F127 : lysine) | Theoretically | | | Experimentally ^a | | |
|-----------------------|-----------------------------|---------------|------------------|--------|-----------------------------|--------|------|
| | | DP of lysine | Block length | M_n | M_n | M_w | PDI |
| Amino-terminated F127 | 1 : 0 | — | 12 600 | 12 600 | 9785 | 13 643 | 1.39 |
| FL-2 | 1 : 4 | 2 | 256–12 600–256 | 13 112 | 10 484 | 15 477 | 1.48 |
| FL-5 | 1 : 10 | 5 | 640–12 600–640 | 13 800 | 11 213 | 15 288 | 1.36 |
| FL-8 | 1 : 16 | 8 | 1024–12 600–1024 | 14 648 | 12 241 | 18 991 | 1.55 |

^a Determined by GPC.

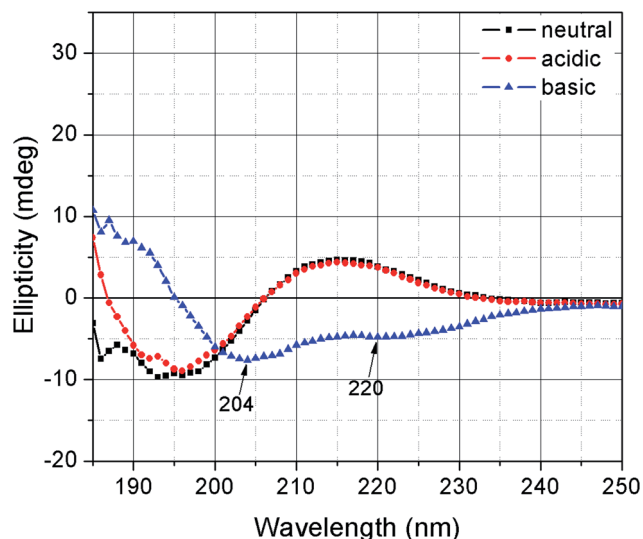


Fig. 2 CD spectra of oligo(lysine)-modified PEG4000 aqueous solution (0.1 wt%) as a function of pH.

indicate that the oligo(lysine) did not readily have a secondary structure due to the low DP of lysine and the short segment. In an acidic and neutral environment, the side chain of lysine was positively charged. The polymer chains stretched due to electrostatic repulsion. Conversely, under alkaline conditions, intramolecular hydrogen bonds could be formed to assemble an α -helix conformation further.^{25,26} The helical arrangement of oligo(lysine) increased the availability of the amino group along the backbone to form intermolecular hydrogen bonds or other subsequent reactions.

Gelation properties

FL hydrogels were obtained by dissolving different mass fractions of FL polymer in deionized water at low temperature and incubating at 37 °C. The hydrogels reverted to the solution state when the ambient temperature decreased below the gelation temperature. The CMT and CGT of the FL hydrogels were determined by DSC and tube inversion, and the values are reported in Table S1.† The CGT obtained by the two methods were consistent. Fig. 3 plots the CMT and CGT measured by DSC. As shown in Fig. 3, the CMT and CGT of all hydrogel groups decreased as the concentration increased, whereas the CMT of

the three groups of FL hydrogels did not considerably differ. These findings indicated that the introduction of oligo(lysine) had no effect on the micellization process. However, the relationship of the CGTs of the hydrogels at the same concentration was as follows: FL-8 > FL-5 > FL-2 > F127. Hence, a high lysine content translated to a high CGT. Among the hydrogels, 16% FL-8 hydrogel had the highest CGT (34 °C).

F127 has a unique “intermediate hydrophobic, hydrophilic at both ends” segment structure. When the temperature was raised, the PPO segments underwent hydrophobic association to form micelles with PPO as the core. The micelles were further rearranged to form hydrogels as the temperature continued to increase.²⁷ Lysine is soluble in water. Modification of F127 with oligo(lysine) altered the hydrophilic–hydrophobic balance in the hydrogel system, thereby increasing the CGT. In addition, the hydration of the amino group on lysine was strong, which weakened the temperature-sensitive effect and even prevented the gelation of the FL polymer. The CGT of the hydrogel became irregular when the DP of lysine was 10, and the hydrogel could not be formed with a continuous increase in the content of lysine. Therefore, the DP of oligo(lysine) designed to modify F127 was set as 2, 5, and 8. In summary, the FL hydrogels had temperature-responsive, adjustable, reversible gelation properties.

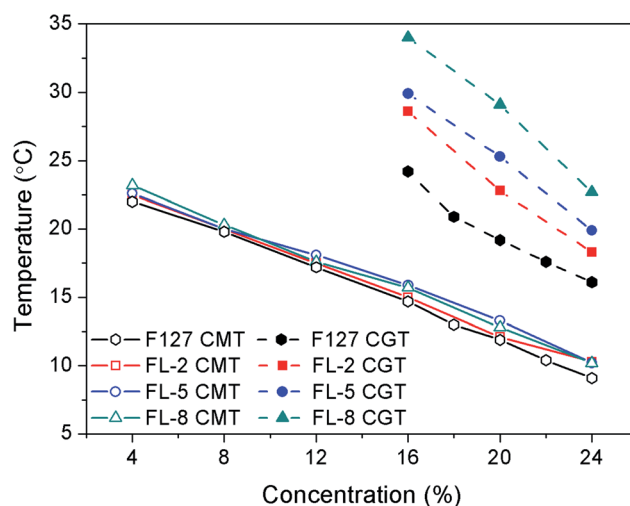


Fig. 3 CMT and CGT of F127 and FL hydrogels measured by differential scanning calorimeter.



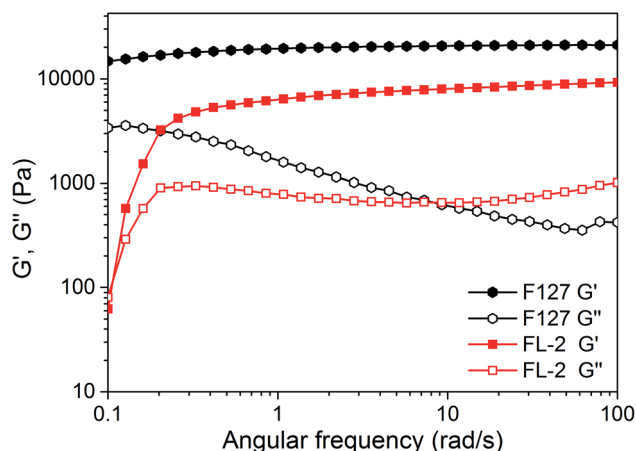


Fig. 4 Storage moduli (G') and loss moduli (G'') of F127 and FL-2 hydrogels at 37 °C.

Rheological properties

The rheological test reflects the mechanical properties of the hydrogel. The storage moduli (G') and loss moduli (G'') of F127 and FL-2 hydrogels were studied by small-deformation oscillatory method, as shown in Fig. 4. At a low frequency regime, the G' of FL-2 hydrogel increased rapidly with increasing frequency. This indicated that FL-2 hydrogel had fluidity at low frequency, and showed the characteristics of reversible gel.²⁸ At a high frequency regime, both hydrogels showed $G' > G''$, F127 and FL-2 hydrogels exhibited the gel state. The G' of F127 hydrogel was about 2×10^4 Pa, and the G' of FL-2 was close to 1×10^4 Pa. The higher G' of the two hydrogels indicated that the polymer network was compact, and high degree of noncovalent cross-linked gels were formed.

Micelles in dilute solution

The structure of lysine theoretically provided a pH-responsive group (amino group). Thus, the micelle size in a FL-5 dilute solution at different pH levels was tested by DLS. Table 2 presents the micelle sizes at pH 3.0, 7.4, and 11.0. The results show that the diameter of the micelles enlarged as the pH increased.

The morphology of the micelles was observed by TEM to explore the state of the micelles further, as shown in Fig. 5. The micelles did not appear to have a complete shape under acidic conditions. When the pH was 7.4, the micelles were spherical and began to aggregate. The average diameter of a single micelle was 16.7 nm. Under alkaline conditions, the micelles continued to aggregate and grew into a rod-like shape, as shown in Fig. 5(c) and (d). The width of the rod-shaped micelles was

Table 2 The average size of the micelles in 0.05 wt% FL-5 solution at different pH values measured by dynamic light scattering ($n = 3$)

| pH | 3.0 | 7.4 | 11.0 |
|-------------------------|------|-----|------|
| Micellar diameters (nm) | 88.5 | 164 | 371 |

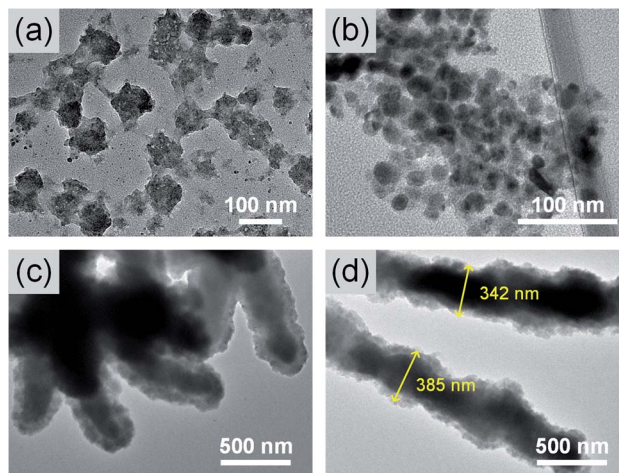


Fig. 5 TEM images of micelles with pH values of (a) 3.0, (b) 7.4, and (c) and (d) 11.0. The FL-5 solution (0.05 wt%) was deposited on to a copper specimen grid and dried overnight at room temperature.

approximately 343 nm. The micelle size observed by TEM was consistent with the results of DLS. Thus, as the pH value increased, the micelle size increased, and aggregation occurred.

As pH increased, the deprotonation of the amino group of lysine caused a change in the concentrations of ions inside and outside the polymer. The number of hydrogen bonds between the oligo(lysine) segments was increased; consequently, the micelle aggregation became increasingly remarkable. In addition, as the pH increased, the secondary structure of oligo(lysine) changed to α -helix, making the structure of the FL polymer more compact than before. The arrangement of the amino groups on the outside of the FL polymer also promoted the formation of intermolecular hydrogen bonds. Thus, the deprotonation of the amino group and the conversion of the secondary structure of the oligo(lysine) resulted in changes in the size and morphology of the micelles in the dilute solution. The FL polymer exhibited pH responsivity.

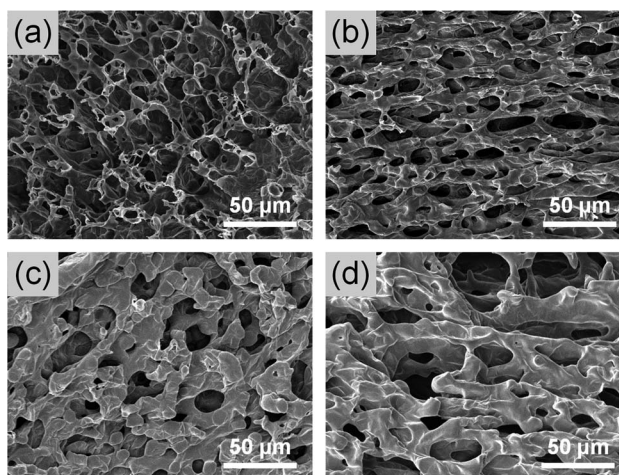


Fig. 6 SEM images of interior morphologies of lyophilized (a) F127, (b) FL-2, (c) FL-5, and (d) FL-8 hydrogels.



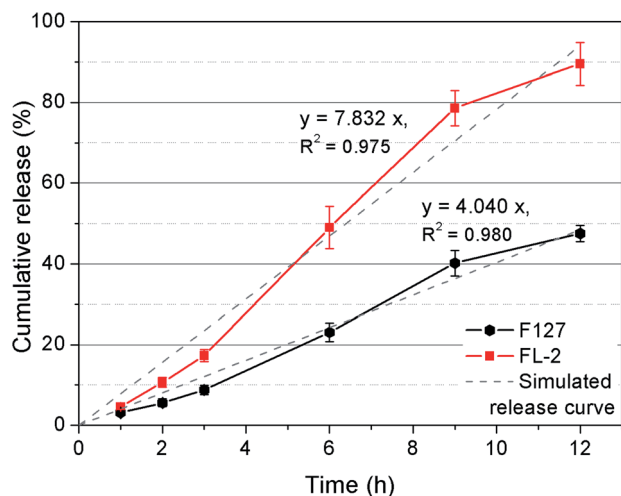


Fig. 7 Release of 5-FU from F127 and FL-2 hydrogels in PBS at 37 °C within 12 hours. Data represent the means \pm SD of 5 replicates.

Interior morphology

Fig. 6 shows the SEM micrographs of freeze-dried 20% F127 hydrogel and FL hydrogels. The interior of all hydrogels exhibited an interconnected porous structure. In Fig. 6(a), the pore walls of the F127 hydrogel were thin, and the pore size was irregular. By contrast, the pores inside the FL hydrogels were ellipsoidal. The porous structure of the FL hydrogel was directional, which was possibly related to the fact that the micelles could be aggregated into a rod-like shape in the TEM results. The pore walls of the FL hydrogel were significantly thicker than

those of the F127 hydrogel. Furthermore, as the lysine content increased, the pores of the FL hydrogel were enlarged, and the pore walls thickened. The average pore wall thickness of the FL-2 hydrogel was 4.84 μm . The pores inside the FL-2 hydrogel had a more complete structure than those inside the other groups of FL hydrogels.

Drug release studies

As shown by the SEM results, the FL-2 hydrogel had the most complete network structure. Therefore, the effect of oligo(lysine) on the sustained release properties of F127 hydrogels was investigated by comparing 20% FL-2 hydrogel with F127 hydrogel. Each group of hydrogels was loaded with 5 mg 5-FU, and their release profile was observed within 12 h. 5-FU is an early anticancer drug that is most widely used in clinical anti-pyrimidine drugs.^{29,30} It has a good therapeutic effect on gastrointestinal cancer and other solid tumors. However, its metabolism in the body may reduce the efficacy. Fig. 7 shows the CR% curves. The two hydrogels exhibited an approximately linear release to 5-FU over the 12 h. In addition, a comparison of the slopes of the simulated release curves shows that the release rate of FL-2 hydrogel was 1.9 times that of the F127 hydrogel. The hydrogels of the two groups reached the maximum release amount at about 12 h, and the release curves within 24 h were shown in Fig. S2.† After 12 h, the CR% of the F127 hydrogel was 47.6%, whereas the CR% of the FL-2 hydrogel was 89.5% (nearly complete release). The results show that the release rate and total release amount of FL-2 hydrogel were larger than those of F127 hydrogel. These were due to two aspects. On the one hand, the SEM images show that the internal pore size of the FL-2

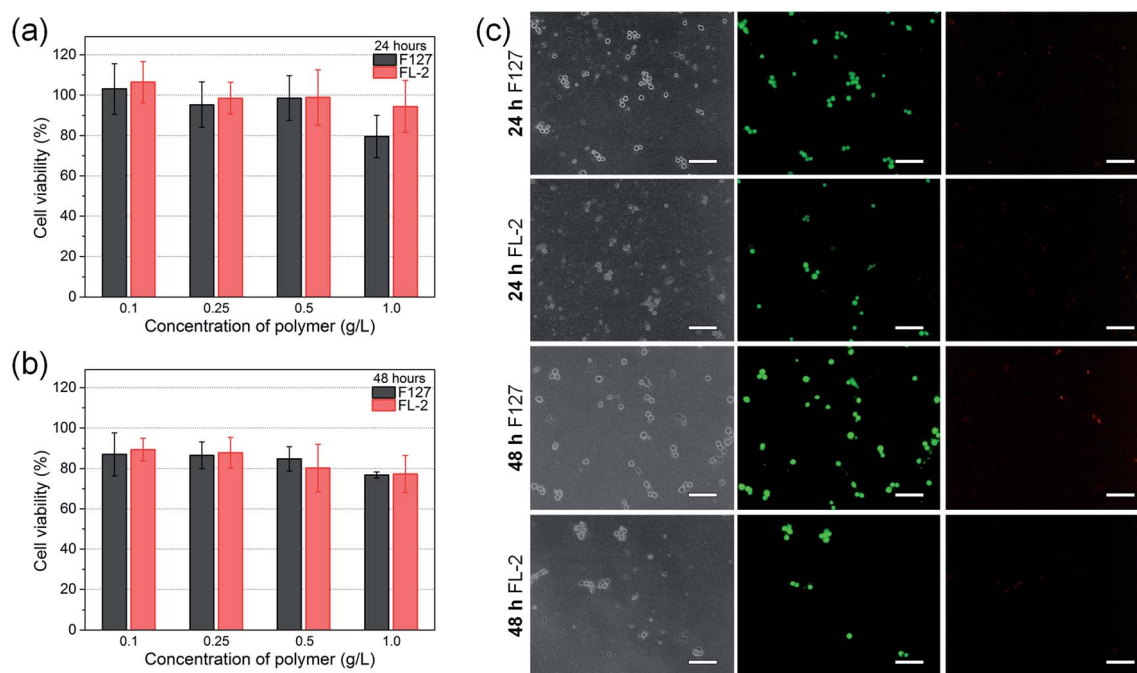


Fig. 8 *In vitro* cytotoxicities of polymer with different concentrations to NIH/3T3 cells in (a) 24 h and (b) 48 h. Data of each group represent the means \pm SD of 6 replicates. (c) Live/Dead staining of NIH/3T3 cells encapsulated in F127 and FL-2 hydrogels for 24 and 48 h (live cells: green, dead cells: red). Scale bars, 100 μm .



hydrogel was large, and the substance exchange speed was fast, which caused the drug lost from the polymer network. On the other hand, the modification of F127 with oligo(lysine) corresponded to the introduction of a hydrophilic component into the hydrogel system. Increasing the hydrophobic component would cause the hydrogel to be easily destroyed in water. Therefore, the drug release may have been achieved by simple diffusion and matrix degradation.

In vitro cytocompatibility evaluations

The cytocompatibility of FL-2 hydrogel to NIH/3T3 cells was evaluated by MTT assay and 3D cell encapsulation and release. As shown in Fig. 8(a) and (b), F127 hydrogel would reduce cell viability due to fast disintegration and material toxicity. As the F127 concentration increased, the cytotoxicity became greater. Overall, the cytotoxicity of FL-2 reduced, which was attributed to the introduction of biomolecule (oligo)lysine. FL-2 at a concentration of 0.1–1.0 g L⁻¹ all showed good biocompatibility. When the FL-2 concentration was 1.0 g L⁻¹, the cell viability of NIH/3T3 cells was still 94.4% and 77.3% after 24 and 48 h. Fig. 8(c) is the images observed with a fluorescence inverted microscope after encapsulating NIH/3T3 cells in hydrogel for 24 and 48 h and staining them with Live/Dead stains. Green represents live cells, and red represents dead cells. Less dead cells were observed in FL-2 hydrogel, which also indicated the low cytotoxicity of FL. Compared with F127 hydrogel, the number of cells encapsulated by FL-2 hydrogel was observed to be smaller. This was due to the disintegration of FL-2 hydrogel in water environment. When cultured for 24 h, the hydrogel was partially degraded, and after 48 h the hydrogel was completely degraded and the cells were all released. FL hydrogel was a physical hydrogel formed by hydrophilic–hydrophobic interaction and hydrogen bonding, so it was not very stable and easily disintegrated. In addition, because the hydrophobic component of lysine was added to FL compared to F127, FL hydrogel was more likely to be destroyed in water. Therefore, (oligo)lysine reduced the cytotoxicity of FL hydrogels, and because of its hydrophobicity, the stability of hydrogels in water was weakened. FL-2 hydrogel had good biocompatibility and cell release behavior, and can be used for cell delivery.

Conclusions

FL was synthesized, and the DPs of lysine were 2, 5, and 8. The reaction was performed at room temperature without the need for a catalyst. FL had a simple linear structure. The molecular weight could be controlled by the distribution ratio and had low polydispersity.

FL had temperature and pH sensitivities. FL hydrogels had reversible temperature-dependent micellization and gelation transitions similar to those of F127. The hydrophilicity of lysine and the hydration of the amino group increased the CGT of the hydrogel with increasing lysine content. The introduction of lysine made the FL hydrogel pH responsive. The secondary structure of oligo(lysine) under alkaline conditions changed into an α -helix. The dilute solution of FL revealed that as the pH

increased, the micelles increased in size and aggregated, eventually growing into a rod-like shape in an alkaline environment. For the internal interpenetrating porous structure, the FL hydrogel had elliptical and thick-walled pores, of which the FL-2 hydrogel was the most complete. 5-FU loaded FL-2 hydrogel could be linearly released within 12 h, and the CR% reached 89.5%. The release mechanism comprised diffusion and matrix degradation. FL-2 had good biocompatibility.

The introduction of lysine not only increased the gel temperature but also made the hydrogel pH sensitive. Moreover, the amino group provided chemical sites for subsequent reactions. Therefore, FL hydrogels are expected to be applied in the biomedicine field, especially in drug and cell delivery systems.

Conflicts of interest

The authors declare no competing financial interest.

Acknowledgements

The authors gratefully acknowledge the financial supports for this research from the Natural Science Foundation of Jilin Province (No. 20180101197jc) and the Program for International S&T Cooperation Projects of China (No. 20190701001GH).

References

- 1 L. Hu, Q. Zhang, X. Li and M. J. Serpe, *Mater. Horiz.*, 2019, **6**(9), 1774–1793.
- 2 X. Li and X. Su, *J. Mater. Chem. B*, 2018, **6**, 4714–4730.
- 3 H. R. Culver, J. R. Clegg and N. A. Peppas, *Acc. Chem. Res.*, 2017, **50**, 170–178.
- 4 L. Klouda and A. G. Mikos, *Eur. J. Pharm. Biopharm.*, 2008, **68**, 34–45.
- 5 L. Klouda, *Eur. J. Pharm. Biopharm.*, 2015, **97**, 338–349.
- 6 P. Alexandridis and T. Alan Hatton, *Colloids Surf., A*, 1995, **96**, 1–46.
- 7 X. Fu, Y. Shen, Y. Ma, W. Fu and Z. Li, *Sci. China: Chem.*, 2015, **58**, 1005–1012.
- 8 J.-Y. Lin, P.-L. Lai, Y.-K. Lin, S. Peng, L.-Y. Lee, C.-N. Chen and I. M. Chu, *Polym. Chem.*, 2016, **7**, 2976–2985.
- 9 H. H. Jung, K. Park and D. K. Han, *J. Controlled Release*, 2010, **147**, 84–91.
- 10 A. Song, A. A. Rane and K. L. Christman, *Acta Biomater.*, 2012, **8**, 41–50.
- 11 E. Ruel-Gariepy and J. C. Leroux, *Eur. J. Pharm. Biopharm.*, 2004, **58**, 409–426.
- 12 K. M. Park, S. Y. Lee, Y. K. Joung, J. S. Na, M. C. Lee and K. D. Park, *Acta Biomater.*, 2009, **5**, 1956–1965.
- 13 E. Bakaic, N. M. B. Smeets and T. Hoare, *RSC Adv.*, 2015, **5**, 35469–35486.
- 14 D. Buenger, F. Topuz and J. Groll, *Prog. Polym. Sci.*, 2012, **37**, 1678–1719.
- 15 S. Murdan, *J. Controlled Release*, 2003, **92**, 1–17.
- 16 J. Z. Hilt, A. K. Gupta, R. Bashir and N. A. Peppas, *Biomed. Microdevices*, 2003, **5**, 177–184.



- 17 A. C. Engler, H.-i. Lee and P. T. Hammond, *Angew. Chem., Int. Ed.*, 2009, **48**, 9334–9338.
- 18 S. Peng, J. Y. Lin, M. H. Cheng, C. W. Wu and I. M. Chu, *Mater. Sci. Eng., C*, 2016, **69**, 421–428.
- 19 S. E. Grieshaber, T. Nie, C. Yan, S. Zhong, S. S. Teller, R. J. Clifton, D. J. Pochan, K. L. Kiick and X. Jia, *Macromol. Chem. Phys.*, 2011, **212**, 229–239.
- 20 H. J. Oh, M. K. Joo, Y. S. Sohn and B. Jeong, *Macromolecules*, 2008, **41**, 8204–8209.
- 21 R. Liu, B. He, D. Li, Y. Lai, J. Chang, J. Z. Tang and Z. Gu, *Int. J. Nanomed.*, 2012, **7**, 4433–4446.
- 22 G. J. M. Habraken, M. Peeters, C. H. J. T. Dietz, C. E. Koning and A. Heise, *Polym. Chem.*, 2010, **1**, 514–524.
- 23 S. Nie, W. L. Hsiao, W. Pan and Z. Yang, *Int. J. Nanomed.*, 2011, **6**, 151–166.
- 24 N. Greenfield and G. D. Fasman, *Biochemistry*, 1969, **8**, 4108–4116.
- 25 Y. P. Myer, *Macromolecules*, 1969, **2**, 624–628.
- 26 H. Noguchi, *Biopolymers*, 1966, **4**, 1105–1113.
- 27 P. Li, C. Zhang, R. Li, L. Qu, X. Dai, Y. Sui and J. Hou, *ACS Appl. Bio Mater.*, 2019, **2**, 527–532.
- 28 M. C. Roberts, A. Mahalingam, M. C. Hanson and P. F. Kiser, *Macromolecules*, 2008, **41**, 8832–8840.
- 29 Y. Arakawa, M. Nakano, K. Juni and T. Arita, *Chem. Pharm. Bull.*, 1976, **24**, 1654–1657.
- 30 L. Li, L. Chen, H. Zhang, Y. Yang, X. Liu and Y. Chen, *Mater. Sci. Eng., C*, 2016, **61**, 158–168.

